Appl Phys A (2008) 93: 399–403
DOI 10.1007/s00339-008-4784-8

Applied Physics A
Materials Science & Processing

RAPID COMMUNICATION

TiO_2 microstructures by inversion of macroporous silicon using atomic layer deposition

A. Langner · M. Knez · F. Müller · U. Gösele

Received: 14 May 2008 / Accepted: 4 June 2008 / Published online: 6 July 2008
© The Author(s) 2008. This article is published with open access at Springerlink.com

Abstract An approach is presented which is capable of fabricating arbitrarily shaped three-dimensional microstructures. Two methods—namely, macroporous silicon and atomic layer deposition—are combined to realize structures in the micrometer and submicrometer range. Using TiO_2 as an example, the fabrication of single hollow objects as well as complex network structures is shown. The scalability and the wide range of applicable materials are the key points of this method for future applications.

PACS 81.05.Rm · 81.15.-z · 82.45.Vp

1 Introduction

During the last decades porous materials have gained a growing importance for applications [1]. Driven by their large surface-to-volume ratio they are especially meaningful for material science and interface chemistry. For the latter, an enhancement of the efficiency of catalytic and ion exchange processes and of adsorbents for gas separation is interesting. Therefore, a high surface-to-volume ratio is a figure of merit for application-driven research. Dependent on their average pore size porous materials can act as ratchets for microspheres [2] or as molecular sieves [3]. Furthermore, porous materials, particularly those with a well defined pore shape and geometry, are widely used as template materials, e.g., for molding polymers [4] or as microreactors [5].

A. Langner (✉) · M. Knez · F. Müller · U. Gösele
Max Planck Institute of Microstructure Physics, Weinberg 2,
06120 Halle (Saale), Germany
e-mail: alangner@mpi-halle.mpg.de

Meanwhile, a broad range of techniques has been established for the fabrication of ordered porous materials [6–12]. However, the controlled growth of uniform structures with reproducible pore shapes is still a challenging task, especially for three-dimensional (3D) geometries. Recently, new approaches towards 3D structures were presented, e.g., direct laser writing by two-photon polymerization [8, 9], holographic lithography [10], and microsphere self-assembly [11]. Although these methods are capable to provide very nice templates, they require high technological effort for shrinkage compensation [12] and are not easily scalable. Furthermore, these processes are limited to only a few materials.

To overcome these limitations we present a new approach towards 3D functionalized porous materials. For this purpose we combine a very versatile 3D etching technique for the preparation of templates with a method ideally suited for the manipulation of surface properties of porous structures. In addition, with this process it is even possible to replicate the entire porous template into a number of different materials.

2 Template fabrication

2.1 Macroporous silicon

As a template material for 3D shaped structures macroporous silicon is used. Since the beginning of the 1990s it has been an intensively studied and well established material system with numerous applications [13]. The etching of pores in silicon is performed via a photo-assisted electrochemical etching process in hydrofluoric acid (HF). As

shown in several publications, two-dimensional pore structures with diameters in the range of a few hundred nanometers up to several micrometers as well as high aspect ratios can be achieved [14]. Moreover, it was shown that this process can be modified in a way suitable for the etching of 3D structures with a precision even sufficient to provide applications as 3D photonic crystals [15].

In this work n-type silicon wafers oriented in ⟨100⟩ direction and with a resistivity of 1 Ω cm are used. Nucleation sites were lithographically defined at the front side of the wafer which is necessary to initialize an ordered pore formation process. A pattern with a square pit arrangement and a distance from pit to pit of 2 µm is used. For the pore etching aqueous HF is taken with a concentration of $c = 5$ wt% at a temperature of $T = 10°\mathrm{C}$. The etching speed is about one micrometer per minute.

The key advantage in this process is the potential to control the porosity during the pore etching by proper adjustment of the backside illumination intensity. Thus, samples with a modulated porosity in all three dimensions can be obtained. The geometry of the templates used in this work can be seen in Fig. 1(a) and 1(b). These scanning electron microscope (SEM) micrographs of the sample's cross section show modulated pores with an interpore distance of 2 µm. The total depth of the sample is 30 µm comprising 17 modulations with a minimum pore diameter of 0.4 µm and a maximum pore diameter of 1.6 µm.

After the etching process in HF the silicon surface is hydrogen-terminated. Storing the sample in normal environment will cause the growth of a layer of native silicon dioxide within a few hours. The thickness of this layer is about three nanometers and remains stable. Due to the humidity of the air the surface is hydroxyl-terminated.

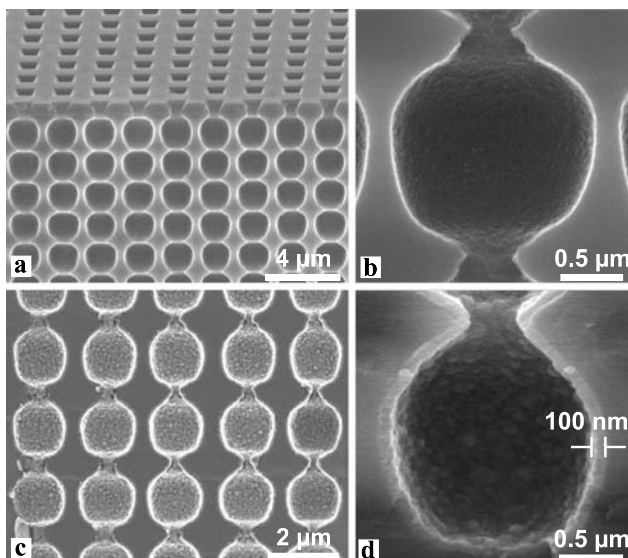

Fig. 1 SEM micrographs of 3D modulated macroporous silicon. (**a**) Bird's eye view of an etched sample with 2 µm interpore distance. (**b**) Cross section of a single modulated pore. (**c**), (**d**) After deposition of 1000 cycles of TiO_2 the pore walls are covered with a 100 nm thick layer of TiO_2

2.2 Atomic layer deposition

For different fields of application of porous templates it is mandatory to gain control over their surface properties. In order to combine this versatile method for the preparation of custom made pore shapes with a large number of different materials and functionalized surfaces we investigated the treatment of our macroporous silicon templates by atomic layer deposition (ALD) [16]. ALD is an improvement of the chemical vapor deposition process with the ability to grow uniform and precisely thickness-controlled films over large areas. Compared to standard chemical or physical vapor deposition techniques ALD works with a self-limiting process using different precursors in an alternating sequence. Although the basic idea of ALD has been known for a few decades it just has been widely used during the last few years to deposit thin films onto complex three-dimensionally structured surfaces. Meanwhile, there are many elements and compounds that can be deposited by ALD, e.g., nitrides, sulfides, metal oxides, and even pure metals [17–19]. Due to its importance as a photocatalytic and bio-degradable material we chose titanium dioxide (TiO_2) as a model system for the deposition of films on the silicon surface [20, 21]. However, this process is not limited to TiO_2: Choosing appropriate reactants a number of chemical elements and compounds can be used to produce a variety of novel microstructures in different materials.

The deposition of TiO_2 was performed following the work of Aarik et al. [22]. For the process a commercial reactor (Savannah100, Cambridge NanoTech Inc.) was used. The two reactants are titanium isopropoxide ($Ti(OCH(CH_3)_2)_4$) and H_2O. The titanium isopropoxide precursor replaces the hydroxyl group remaining on the surface of the macroporous silicon under abstraction of isopropanol. Subsequently, the remaining alcoholate is hydrolyzed with H_2O. After complete hydrolysis the surface is again hydroxyl-terminated, allowing for repeated reaction. The temperature in the reaction chamber was 150°C and the half-cycle time for each precursor was chosen to be 90 s. Between every precursor pulse the chamber was purged to remove excess material and reaction by-products.

In contrast to the deposition of films on flat surfaces, the reactants had to diffuse into the porous structure and therefore the exposure time had to be adapted. A sufficiently long exposure time ensures homogeneous growth over the whole pore depth due to homogeneous distribution of the precursor material across all accessible surfaces.

In Fig. 1(c) and 1(d) the result of the coating process is shown for the sample in Fig. 1(a) and 1(b). The layer of TiO_2 can be identified by the difference in contrast (Fig. 1(d), brighter film on top of the silicon). The layer thickness was measured to be 100 nm. All in all, 1000 cycles were performed, and thus the growth rate can be estimated to 0.1 nm per cycle.

Although on the surface the titanium dioxide agglomerates into a grain structure the thickness of the film is highly conformal within the pores. In fact, no difference in thickness could be measured for the deposited layer of the first and the last pore modulation. This means that the precursor exposure times were sufficient to ensure a uniform deposition of material along the pore wall, and thus it indicates a successful growth within the self-terminating ALD reaction regime.

For the grain structure a reasonable explanation can be found: Presumably, the growth of a smooth layer is hindered due to an initial island growth (supported by the surface roughness of the macroporous silicon) and the formation of polycrystalline anatase films which is expected at those temperatures (150°C). Depending on later applications the grain size and therefore the surface roughness can be significantly reduced, e.g., by a short oxidation followed by an HF-dip prior to the ALD. Beside this change in surface preparation, lower or higher process temperatures in the ALD reactor are possible and therefore different crystal phases of TiO_2 or amorphous TiO_2 can be obtained. The latter would result in smoother layers as well.

3 Results

3.1 Single microstructures

Because of the uniform coating, which is a significant advantage of the ALD process, the etched silicon pore structure is completely reproduced into the coating material. To make this visible the silicon was removed selectively in an aqueous solution containing 10 wt% potassium hydroxide (KOH). The KOH etches the silicon at a rate of 1.5 μm per hour at room temperature [23]. It is worth to mention that part of the deposited TiO_2 had to be removed prior to the KOH step (e.g., by scratching or polishing the surface or cleaving the sample). Otherwise, the KOH cannot dissolve the silicon since the whole surface is protected by TiO_2. A scheme of the whole process is shown in Fig. 2(a). In the initial silicon (light blue) with predefined etch pits a modulated structure is etched. With ALD, a layer of TiO_2 (red line) is coated and after several hours in KOH the silicon is completely dissolved. What remained are chains of connected hollow titanium dioxide spheres as displayed in Fig. 2(b)–2(d). The chains are very uniform in size and shape, which proves the ability of the presented process to fabricate millions of equally shaped microstructures.

Furthermore, single spheres can be obtained, too. For that purpose the small connecting part between the spheres has to be cracked. Since this is the most fragile part of the structure it will break preferentially at this part when an external force is applied, e.g., by ultrasonic exposure (Fig. 2(d)). The surface of these single spheres seems to be furry. Because

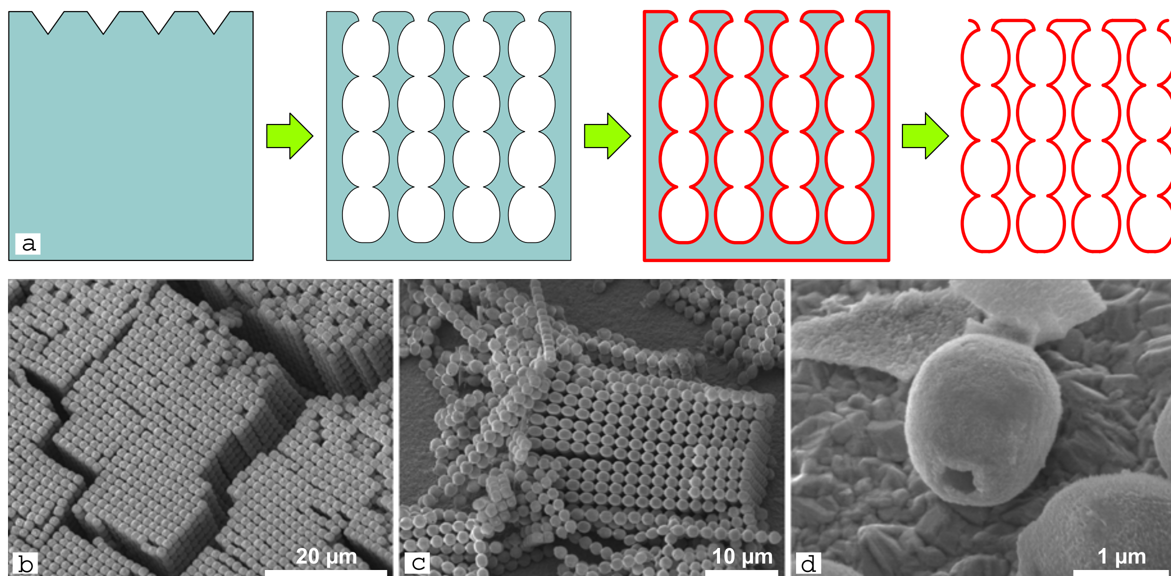

Fig. 2 From macroporous silicon template to TiO_2 microstructures. (**a**) Scheme of the reproduction process: The initial silicon (*light blue*) with predefined etch pits is etched. After coating the surface with ALD (*red line*) and selectively removing the silicon in KOH, pure TiO_2 microstructures remain. (**b**) An array of hollow TiO_2 micropearl chains viewed from the bottom and (**c**) from the side. (**d**) Single isolated TiO_2 micropearls as a perfect copy of the inner surface of the original macroporous silicon structure

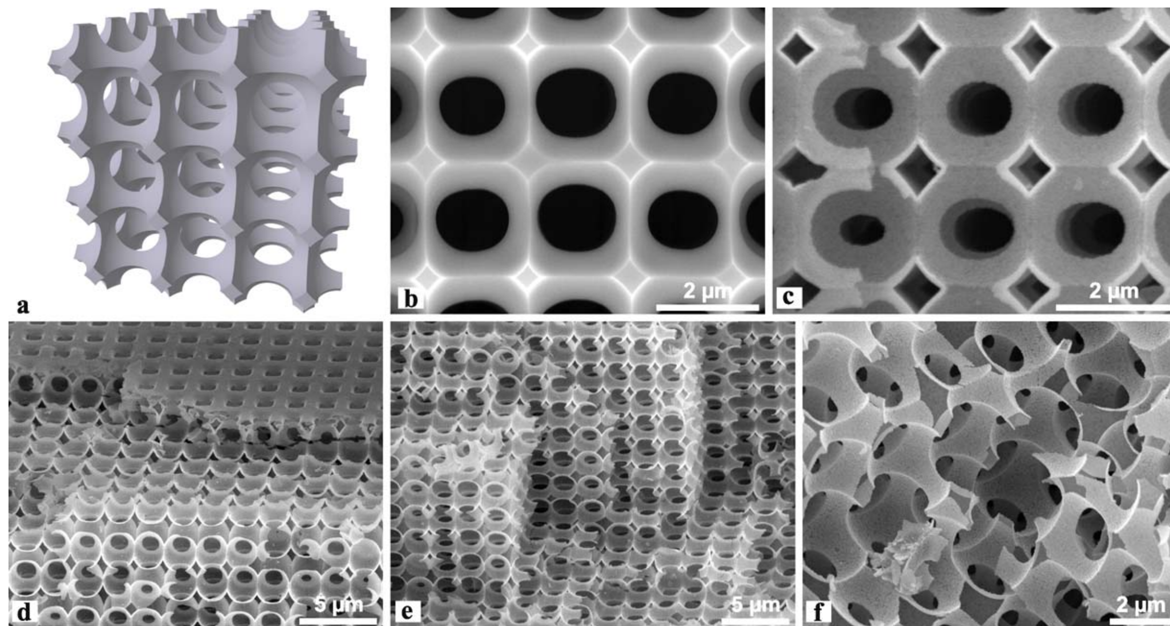

Fig. 3 Porous network structures. (**a**) 3D model of the network structure of connected air spheres. (**b**) SEM micrograph of the pore cross section of silicon after the widening procedure. The *gray* parts are the remaining silicon with sharp edges (*bright lines*) and connected to each other. In the *dark* areas the silicon is completely removed and therefore an opening to the neighboring pore is established. After the replication of the silicon structure highly porous TiO_2 network structures are obtained: (**c**) Cross sectional view. (**d**) Bird's eye view where part of the top layer is removed. (**e**), (**f**) A closer look into the porous TiO_2 scaffold structure

of the molding process the inner surface of the macroporous silicon is reflected in the outer surface of the TiO_2 sphere. This feature can be used to obtain a measure of the surface roughness of the macroporous silicon pores.

3.2 Network structures

Hitherto, after removing the silicon the modulated TiO_2 tubes were sticking together just by weak adhesion force. Nevertheless, for reasons of stability as well as device applications arrays of interconnected pores are useful as well. For instance, porous structures for enhanced catalytic reactions or cell culturing applications, especially in 3D [24].

The realization of such interconnected 3D network structures is described in the following: Starting from a modulated pore shape as shown in Fig. 1(a) an additional treatment prior to the ALD process is carried out. In order to connect the pores in the lateral direction as well, the thin part of the walls between neighboring pores has to be removed. This is accomplished by a combination of oxidation and subsequent removal of the silicon dioxide in NH_4F (12.5 wt%). In order to minimize the induced stress during the oxidation caused by the difference in the volume fractions of Si and SiO_2 this pore widening procedure is split into four steps. Every step consists of four hours oxidizing at 950°C in ambient atmosphere and one hour etching in NH_4F. Thereby, the oxidation time determines the amount of silicon that is oxidized. The subsequent treatment in NH_4F selectively etches only the SiO_2, and thus the pores are widened in diameter up to the point where they get connected to each other. For better visualization a 3D model of this structure is provided in Fig. 3(a). The pore cross section after the widening procedure is shown in Fig. 3(b): In the dark areas a connection with the neighboring pore is established.

The subsequent treatment with the described ALD process and dissolution of the silicon results in highly porous network structures as can be seen in Fig. 3(c)–3(f). The shape of the original silicon scaffold structure is perfectly reproduced in TiO_2 with a wall thickness of only a few ten nanometers. Although this structure is highly porous with an air filling ratio of more than 85% it is stable because of the homogeneously etched template and the deposited TiO_2 layer. Likewise, the surface area was increased by a factor of 2 because now both sides of the TiO_2 wall can be used for exposure or as reactant area.

4 Conclusion

In conclusion, a new process was presented to achieve 3D microstructures and porous network structures. For possible applications the presented TiO_2 micropearls are well suited as carriers for drug delivery, whereas the network structures can work as highly porous photocatalytic material. Macroporous silicon as template material offers the possibility to achieve variously shaped microstructures in two and even

three dimensions. Since the etching process is a parallel one, it can be scaled up easily to common wafer sizes and thus billions of identical copies of a designed shape can be grown on a large scale.

Furthermore, we applied ALD as a deposition technique because the self-terminating process is well suited to cover porous materials where material diffusion has to be taken into account. This is especially meaningful for the high aspect ratios of several hundreds that can be obtained with macroporous silicon. In addition, many different materials and compounds can be used in the ALD process so that the properties of the surface are highly flexible and can be designed for specific applications. In contrast to polymer-based template fabrication methods, structures etched in macroporous silicon can be used as templates for even higher process temperatures during the ALD process. The combination of these two methods delivers a broad variety of custom-shaped porous templates with functionalized surfaces beyond commonly available templates.

Open Access This article is distributed under the terms of the Creative Commons Attribution Noncommercial License which permits any noncommercial use, distribution, and reproduction in any medium, provided the original author(s) and source are credited.

References

1. M.E. Davis, Nature **417**, 813 (2002)
2. S. Matthias, F. Müller, Nature **424**, 53 (2003)
3. D. Zhao, J. Feng, Q. Huo, N. Melosh, G.H. Fredrickson, B.F. Chmelka, G.D. Stucky, Science **279**, 548 (1998)
4. S. Grimm, K. Schwirn, P. Göring, H. Knoll, P.T. Miclea, A. Greiner, J.H. Wendorff, R.B. Wehrspohn, U. Gösele, M. Steinhart, Small **3**, 993 (2007)
5. L. Zhao, N. Li, A. Langner, M. Steinhart, T.Y. Tan, E. Pippel, H. Hofmeister, K.-N. Tu, U. Gösele, Adv. Funct. Mater. **17**, 1952 (2007)
6. V. Lehmann, H. Föll, J. Electrochem. Soc. **137**, 653 (1990)
7. W. Lee, R. Ji, U. Gösele, K. Nielsch, Nat. Mater. **5**, 741 (2006)
8. M. Deubel, G.V. Freymann, M. Wegener, S. Pereira, K. Busch, C.M. Soukoulis, Nat. Mater. **3**, 444 (2004)
9. S. Passinger, M.S.M. Saifullah, C. Reinhardt, K.R.V. Subramanian, B.N. Chichkov, M.E. Welland, Adv. Mater. **19**, 1218 (2007)
10. M. Campbell, D.N. Sharp, M.T. Harrison, R.G. Denning, A.J. Turberfield, Nature **404**, 53 (2000)
11. A.-P. Hynninen, J.H.J. Thijssen, E.C.M. Vermolen, M. Dijkstra, A.V. Blaaderen, Nat. Mater. **6**, 202 (2007)
12. D.C. Meisel, M. Diem, M. Deubel, F. Pérez-Willard, S. Linden, D. Gerthsen, K. Busch, M. Wegener, Adv. Mater. **18**, 2964 (2006)
13. V. Lehmann, *Electrochemistry of Silicon* (Wiley-VCH, Weinheim, 2002)
14. H. Föll, M. Christopherson, J. Carstensen, G. Hasse, Mater. Sci. Eng. R **39**, 93 (2002)
15. S. Matthias, F. Müller, C. Jamois, R.B. Wehrspohn, U. Gösele, Adv. Mater. **16**, 2166 (2004)
16. T. Suntola, J. Antson, US Patent 4 058 430 (1977)
17. R.L. Puurunen, J. Appl. Phys. **97**, 121301 (2005)
18. M. Knez, K. Nielsch, L. Niinistö, Adv. Mater. **19**, 3425 (2007)
19. Z. Li, A. Rahtu, R.G. Gordon, J. Electrochem. Soc. **153**, C787 (2006)
20. M.R. Hoffmann, S.T. Martin, W. Choi, D.W. Bahnemann, Chem. Rev. **95**, 69 (1995)
21. U. Diebold, Surf. Sci. Rep. **48**, 53 (2003)
22. J. Aarik, A. Aidla, T. Uustare, M. Ritala, M. Leskelä, Appl. Surf. Sci. **161**, 385 (2000)
23. H. Seidel, L. Csepregi, A. Heuberger, H. Baumgärtel, J. Electrochem. Soc. **137**, 3612 (1990)
24. N.W. Choi, M. Cabodi, B. Held, J.P. Gleghorn, L.J. Bonassar, A.D. Stroock, Nat. Mater. **6**, 908 (2007)